The Up-regulation of Carbonic Anhydrase Genes of Bacillus mucilaginosus under Soluble Ca^{2+} Deficiency and the Heterologously Expressed Enzyme Promotes Calcite Dissolution

Leilei Xiao[a], Jianchao Hao[a], Weiying Wang[a], Bin Lian[a], Guangdong Shang[a], Yunwen Yang[a], Congqiang Liu[b] & Shijie Wang[b]

[a] Jiangsu Key Laboratory for Microbes and Functional Genomics, Jiangsu Engineering and Technology Research Center for Microbiology, College of Life Sciences, Nanjing Normal University, Nanjing, China

[b] State Key Laboratory of Environmental Geochemistry, Institute of Geochemistry, Chinese Academy of Sciences, Guiyang, China

PLEASE SCROLL DOWN FOR ARTICLE

Taylor & Francis
Taylor & Francis Group

The Up-regulation of Carbonic Anhydrase Genes of *Bacillus mucilaginosus* under Soluble Ca^{2+} Deficiency and the Heterologously Expressed Enzyme Promotes Calcite Dissolution

LEILEI XIAO[1], JIANCHAO HAO[1], WEIYING WANG[1], BIN LIAN[1]*, GUANGDONG SHANG[1], YUNWEN YANG[1], CONGQIANG LIU[2], and SHIJIE WANG[2]

[1]*Jiangsu Key Laboratory for Microbes and Functional Genomics, Jiangsu Engineering and Technology Research Center for Microbiology, College of Life Sciences, Nanjing Normal University, Nanjing, China*
[2]*State Key Laboratory of Environmental Geochemistry, Institute of Geochemistry, Chinese Academy of Sciences, Guiyang, China*

Molecular mechanisms and gene regulation are of interest in the area of geomicrobiology in which the interaction between microbes and minerals is studied. This paper focuses on the regulation of the expression of carbonic anhydrase (CA) genes in *Bacillus mucilaginosus* and the effects of the expression product of the *B. mucilaginosus* CA gene in *Escherichia coli* on calcite weathering. Real-time fluorescent quantitative PCR (RT-qPCR) was used to explore the relationship between CA gene expression in *B. mucilaginosus* and promotion of calcite dissolution under condition of Ca^{2+} deficiency. The results showed that adding calcite to the medium, which lacks Ca^{2+}, can up-regulate the expression of the bacterial CA genes to accelerate calcite dissolution for bacterial growth. CA genes from *B. mucilaginosus* were transferred into *E. coli* by cloning. We then employed crude enzyme extract from the resultant *E. coli* strain in calcite dissolution experiments. The enzyme extract promoted calcite dissolution. These findings provide direct evidence for the role of microbial CA on mineral weathering and mineral nutrition release.

Keywords: *Bacillus mucilaginosus*, Ca nutrition acquisition, carbonic anhydrase, geomicrobiology, heterologous expression, RT-qPCR

Introduction

Mineral weathering can cause the migration of mineral elements (Alekseev et al. 2003; Meunier et al. 2007) and affect geochemical processes (Godderis et al. 2010; Hazen et al. 2008). Physical weathering, chemical weathering and biological weathering are the three main forms of mineral weathering (Warscheid and Braams 2000; Wilson 2004). However, biological weathering involves biochemical and physical processes, such as the secretion of organic acids (McMaster 2012; Neaman et al. 2005; Valix et al. 2001), complexation (Koretsky 2000; Lian et al. 2008b), oxidation-reduction (Brown et al. 2003; Shelobolina et al. 2012; Shock 2009) and bio-mechanical action (Bonneville et al. 2011; Chen et al. 2000). Some materials secreted by organisms has made it easy to identify associations between biological enzymes and

mineral weathering (Fru 2011; Xiao et al. 2012a) and to determine whether organisms can affect the weathering rate through enzyme secretion.

Carbonic anhydrase (CA) is widely distributed in animal cells (Jackson et al. 2007; Supuran and Scozzafava 2007), plant cells (Bradfield 1947; Moroney et al. 2001; Sunderhaus et al. 2006) and microorganisms (Bahn et al. 2005; Hewett-Emmett and Tashian 1996; Smith and Ferry 2000). It is capable of catalyzing the hydration reaction of atmospheric and self-generated CO$_2$ and the reverse reaction $CO_2 + H_2O \Leftrightarrow H^+ + HCO_3^-$ (Meldrum and Roughton 1933; Smith and Ferry 2000; Tripp et al. 2001; Xu et al. 2008). H$^+$ can promote the dissolution of carbonate rocks, which, in turn, affects the CO$_2$ cycle. CA from bovine erythrocytes can affect the dissolution of carbonate minerals in phosphate ores under acidic conditions (Papamichael et al. 2002). The dissolution rate for limestone increases about 10-fold at high p_{CO_2} values after addition of bovine carbonic anhydrase (BCA) (Liu et al. 2005). With dolomite, the dissolution rate with BCA increases about 3-fold at low p_{CO_2} values. These results suggest that the degree of acceleration of carbonate dissolution by CA is different between limestone and dolomite. Demir et al. (2012) also showed that BCA is able to promote

dolomite dissolution. However, this evidence is insufficient to conclude that CA plays an important role in biogeochemical processes on the Earth's surface in general.

The weathering in which microorganisms participate is partly related to their need for mineral elements (Mailloux et al. 2009). Because of the great variety, wide distribution and very active metabolisms of these organisms, microorganism-induced weathering of minerals and rocks has attracted a great deal of attention (Jacobson and Wu 2009; Lepleux et al. 2012; Luttge and Conrad 2004; Shirokova et al. 2012; Stockmann et al. 2012; Uroz et al. 2007). CA genes are present in almost all organisms (Venta et al. 1983), so the study of the function of CA on mineral weathering appears to be very important. Xiao et al. (2012b) showed that a higher expression level of the *Aspergillus fumigatus* CA gene favored weathering of potassium-bearing rocks. They speculated that CA might promote generation of H_2CO_3, promoting weathering of silicate minerals and facilitating the release of K^+. CA can be detected in different soils in the Karst region (Li et al. 2005b). This suggests that CA is widely distributed in the soil of Karst areas. Li et al. (2005a) detected microbial CA activity in column-built leached soil-limestone Karst systems. They surmised that CA secreted from microbes might be a major factor influencing the release of Ca^{2+} in natural systems. In addition, microbial extracellular CA could accelerate the release of Ca^{2+} from limestone (Li et al. 2007; 2009). These results implied that microbial CA might have a significant influence on the bio-karst process. In Li's experiments, a crude enzyme solution containing CA was made from cell secretions. The composition of the solution was very complex. Other substances, such as organic acids, may have affected limestone dissolution. This made it difficult to determine the contribution of each component of the microbial secretions to limestone dissolution. Zhang et al. (2011) showed that CA activity increased as the amount of limestone in the medium increased. This increasing trend was limited only within a certain range, and enzyme activity did not directly reflect the relationship between the expression of CA and mineral weathering. Although the basis for mineral weathering by microbial CA was investigated in earlier studies, some aspects need clarification. Genomes of mineral weathering microbes generally contain several CA genes, it is unclear whether these genes are different from each other, whether all of them are relevant to mineral weathering and, if so, whether their respective gene products exhibit CA activity. To resolve these issues, molecular biology must be used to study the relationship between the expression and regulation of microbial CA genes and mineral weathering. Molecular biology can also be used to analyze the activity of the product of any single CA gene.

Real-time fluorescence quantitative PCR (RT-qPCR) can be used to detect gene expression at specific times (Iskandar et al. 2004; Nolan et al. 2006). An *E. coli* expression system, which is the most common type of expression system, was used in the present study (Banerjee et al. 2009; Small et al. 2010; Sorensen and Mortensen 2005). The *E. coli* expression system is preferred because of its low cost, high productivity and easy operation. An in-depth study of the function of

almost any gene can be performed by combining RT-qPCR and *E. coli* expression.

In our research group, we often use *Bacillus mucilaginosus* to study the interactions between microbes and minerals (Mo and Lian 2011; Xiao et al. 2012a). Zhang et al. (2011) showed *B. mucilaginosus* can capture atmospheric CO_2 by carbonic anhydrase. Alternatively, this strain is widely used in China and surrounding countries as a plant growth-promoting rhizobacterium (PGPR) (Singh et al. 2010) and can be used as fertilizer. The *B. mucilaginosus* K02 genome (GenBank database accession number: HM579819) was sequenced and five CA related genes (Gene ID were 12734710, 12739330, 12735171, 12735237 and CP003422 region: 5453463-5454707) were annotated. RT-qPCR was used to explore the relationship between gene expression and mineral weathering. Five gene amplification products were transferred into *E. coli*, forming recombinant strains. The enzymatic activity of heterologously expressed proteins was determined, and the protein showing the highest activity was selected for calcite dissolution experimentation. The results showed that CA genes expression responds to soluble calcium deficiency and that heterologously expressed protein plays a role in calcite dissolution. The CA genes also provide a new means of investigating the role and regulatory mechanism of microbial CA in biogeochemical processes.

Materials and Methods

Real-time Fluorescent Quantitative PCR

Preparation of calcite powder

Calcite was selected as a typical representative mineral of carbonate rocks. The calcite, from a Karst region of Guizhou province of China, was crushed and a greater than 200-mesh fraction was collected by sieving. The calcite powder was washed by suspension in sterilized ultrapure water (SUW) to eliminate the fine dust from the grinding procedure. The powder was then rinsed three times with ethyl alcohol. The cleaned powder was dried in a convection oven. X-ray diffraction analyses were carried out to identify the mineralogical composition (not shown here). The results showed it was almost pure calcite.

RT-qPCR

RT-qPCR was used to determine whether the calcite could promote the expression of all five CA genes of the. *B. mucilaginosus* strain. Control cultures of *B. mucilaginosus* were grown in nitrogen-containing medium having the following composition per liter: sucrose 10.0 g, $(NH_4)_2SO_4$ 1.0 g, $CaCl_2$ 0.44 g, $MgSO_4$ 0.5122 g, KCl 0.1 g, and $Na_2H-PO_4 \cdot 12H_2O$ 2.507 g. Experimental cultures were grown in the same medium, except that the 0.44 g of $CaCl_2$ were replaced by 0.2 g powdered calcite. After 2 d, 4 d or 6 d of culture, the bacteria were centrifuged ($11500 \times g$, $4°C$, 1 min).

The supernatant was discarded, and the collected cell was frozen in liquid nitrogen. Total RNA was extracted (Invitrogen, following the manufacturer's instruction) and reverse transcribed into cDNA. The RT-qPCR reaction system and

reaction conditions followed the manufacturer's instructions of TaKaRa. As an internal reference, 16S rRNA was used (Table S1). The Ct value was recorded for subsequent analysis. After optimizing the primers by testing different primers, a single melting temperature was determined for each of the 6 pairs of primers (not shown here). The mean of $_{\Delta\Delta}$Ct was set as zero when the bacteria were cultured using the only calcium source, $CaCl_2$, on the second day. The relative expression level (REL) was calculated using the following formula: $REL = 2^{-\Delta\Delta Ct}$.

Construction of Transformants

To verify that heterologously expressed CA can promote calcite dissolution, five clones of all of the CA genes were constructed. A modified SDS-CTAB method (Niu et al. 2008) was utilized to extract genomic DNA because of the secreted extracellular polysaccharide. PCR was performed as described in the molecular cloning section (Sambrook and Russell 2002). The forward and reverse primers (ps1, ps2, ps3, ps4, and ps5) were designed with Primer Premier 5.0. They are listed in Table S2. The amplified fragments were named TCA1, TCA2, TCA3, TCA4, and TCA5. For *in vitro* amplification, PCR was performed in accordance with the manufacturer's instructions for DNA polymerase (Sangon Biotech (Shanghai) Co., Ltd.). The identities of the PCR products were verified using agarose gel electrophoresis. Plasmid pET30a (+), which contained the kanamycin resistance gene (Kan^R), was used as the vector. The purified PCR products were digested at the Kpn I and Hind III sites introduced by the primers and then inserted into Kpn I and Hind III-restricted pET30a (+) to create pXLL01, pXLL02, pXLL03, pXLL04 and pXLL05. Recombined plasmids were transferred into competent cells to form transformants. Five kinds of plasmids were digested with restriction enzymes to confirm whether the recombinant plasmids were correct. Finally, the recombinant plasmids were sequenced.

Protein Expression, Verification and Determination of Protein Activity

The pET30a (+) and five types of recombined plasmids were transferred into *E. coli* BL21 (DE3) competent cells. After isopropyl β-thiogalactopyranoside (IPTG) induction, cultivation was continued for an additional 6 h. Sodium dodecyl sulfate polyacrylamide gel electrophoresis (SDS-PAGE) was used to verify protein expression. One mL of culture solution was centrifuged (16,200 × g, 4°C, 5 min). The supernatant was discarded and the cell precipitate was re-suspended in 300 μL lysis buffer (1 mM EDTA and 20 mM Tris-HCl, pH 8.0). The cell wall was broken by ultrasonication in 3 × 10 s at 10 s intervals. One hundred microliters of suspension was transferred to a clean centrifuge tube and the remainder was centrifuged as described above. The loading buffer (2×; /L: 1 M Tris-HCl [pH 6.8] 100 mL DTT 3 g, 10% SDS 400 mL, Bromophenol blue 2 g, glycerol, 240 mL) was added to the suspension and the supernatant in a volume ration of 1:1, respectively).

All proteins and the marker were treated at 95°C for 5 min. SDS-PAGE was performed using a modified version of the SDS-PAGE Laemmli protocol. Proteins were stained using Coomassie brilliant blue R-250. Decoloration was performed until the band appeared clear. For Western blot analysis, after the samples were electrophoresed, proteins were transferred onto polyvinylidene difluoride (PVDF) membranes for immunoblotting. The membrane was blocked, and the blots were probed with double antibodies. The membrane was immersed in TMB substrate and kept in the dark for 10 min. Finally, protein bands were visualized on PVDF membranes.

Enzyme activity was measured by a method reported in a previous study (Pocker and Stone 1967). Phosphate buffer was prepared at different pH values (6.5, 7.0, 8.0, 9.0 and 9.5). The preparation process for crude enzyme solution (CES) from 90 ml of bacterial suspension followed the description mentioned above for protein preparation. Lysis buffer was replaced by SUW and 2 ml cell resuspension solution was broken by ultrasonication in 6 × 10 s at 10 s intervals. The enzyme activity was calculated by the optical density (OD) value of the color of the product of the enzyme reaction. When OD was determined, the OD value of the reaction solution containing CES, which was from the *E. coli* containing pET30a, was set at zero as the control. Then the enzyme activities of CESs from five recombinants were determined.

Calcite Dissolution

First, 0.0500–0.0505 g of powdered calcite was added to the 100 mL volume flask in three replicates. CES was obtained from the ultrasonication of *E. coli* containing pET30a (+) and pXLL04, named CA0 and CA4, respectively. CA0 and CA4 were obtained using the method described above (protein activity section). It is clear that CA0 only contain CA from expression of *E. coli* genome rather than heterologous expression. Fifty milliliters of SUW containing 200 μL of BCA (2.5 × 10^{-6} g/mL), CA0 or CA4 were added to the flasks named as the BCA group, CA0 group and CA4 group, respectively. Finally, the flasks were placed in a rotary shaker (140 rpm, 35°C).

After 0 min, 10 min, 20 min, 30 min, 60 min, 120 min and 240 min, three flasks containing calcite particle suspension with CA0 and three others containing calcite particles with CA4 were sacrificed and their content filtered by use of separate 0.45 μm filter membranes. The remaining reaction solution was discarded after sampling. The Ca^{2+} in the 20 mL filtered reaction solution from the controls and experimental setups was titrated using ethylenediaminetetraacetic acid disodium salt (EDTA-Na$_2$) referring to pulished literature (Nielsen 2010). Because the calcite was 99% pure, containing just a small amount of quartz, and because the Mg^{2+} in the system did not interfere with the analysis, the titer of EDTA-Na$_2$ was taken to indicate the concentration of Ca^{2+} in a sample. The relative dissolving-out quantity of Ca^{2+} was set as zero at 0 min. At 5 min and 180 min, calcite particles, in the reaction system with CA4 (CA4

group), were taken out and rapidly dried for microscopic examination.

Results

Relationship between the Expression of B. mucilaginosus *CA Genes and Calcite Weathering*

The experiment was designed to explore whether calcite can induce the expression of CA genes by comparing the gene expression quantity of *B. mucilaginosis* cultured in a medium containing calcite (insoluble calcium) with a gene expression quantity of the same strain cultured in a medium containing soluble calcium. The mRNA relative expression quantities of different CA genes are shown in Figure 1.

Overall, variations in expression trends were similar for all five CA genes. In the experimental group (containing calcite without $CaCl_2$), REL gradually improved from the 2nd to the 6th day. However, the REL values for the controls (containing $CaCl_2$ without calcite) remained in the single digit range and did not differ significantly. The REL between experimental and control was as great as two orders of magnitude because of the difference in the source of calcium.

Cloning of CA Genes, Protein Expression and the Determination of CA Activity

The *B. mucilaginosus* K02 genome was extracted. All five types of CA genes were amplified and the bands of their PCR products were identified in 1% agarose gels (Figure S1A). The positions of the bands representing the lengths of the genes were consistent with the calculated values. The recombinant plasmids were constructed by linking the PCR products and digested plasmid pET30a and then they were transferred into competent cells. The recombinant plasmids were extracted and verified by double-enzyme digestion. The sizes of the two bands were consistent with the calculated values (Figure S1B). The sequences of the inserted DNA were determined. The results showed that the target sequences were inserted into the vector plasmids without even one mutated base (data not shown).

The expression systems were constructed by transferring recombinant plasmids into *E. coli* BL21. In brief, in order to facilitate description, proteins were expressed in hosts containing pXLL01, pXLL02, pXLL03, pXLL04 and pXLL05. These proteins are here called PCA1, PCA2, PCA3, PCA4 and PCA5, respectively. The total proteins and supernatant proteins were visualized using SDS-PAGE (Figure 2A). The results showed that the molecular weight of the proteins ranged from 25 kDa to 55 kDa. This was consistent with calculated values, so it can be used as preliminary evidence that these proteins were target proteins. In the five recombinants, PCA3 was most plentiful and PCA5 was least plentiful. The solubilities of these five types of proteins were significantly different. PCA4 showed the most solubility and PCA5 showed the least. Although many inducing conditions (temperature: 25°C and 30°C, final IPTG concentration: 0.1, 0.7

and 1 mM) were explored, an expression gap still remained, indicating the different levels of expression of these five types of CA genes. Codon preference of *E. coli* is likely the reason why there exists the expression gap.

Under the control of the T7 promoter, recombinants were found to produce His-tagged proteins, which are capable of combining with antibodies. Western blots were used to further confirm whether these proteins were target proteins. Poorly soluble proteins were more likely to produce false positives; therefore, these proteins were used in Western blot analysis (Figure 2B). Although PCA3 showed the highest expression levels, its poor solubility was obvious (Figure 2A). PCA3 and PCA5 were selected for further experiments. The levels of these proteins were determined. Their size was found to be consistent with the results of SDS-PAGE (Figure 2A). These proteins were again shown to be the target proteins. The appearance of several untargeted bands may be attributed to expressed His-tagged proteins native to *E. coli*.

A standard curve for the CA activity assay was constructed. The equation of the standard curve was $y = 9.426 \times x - 0.0134$, and the coefficient of correlation was 0.99546. The activity of expressed proteins from the recombinants was determined. All five kinds of proteins showed CA activity (Figure 3) indicating that they were not evolutionary junk. PCA5 demonstrated only limited activity, possibly because it formed only small amounts and these had low solubility. CA4 showed high amounts of enzymatic activity in either acidic or alkaline environments. The maximum activity of CA4, 109.2 mU/mL, was observed at pH 9.0. Variations in enzymatic activity were observed in repeated experiments, but CA4 consistently demonstrated the highest enzymatic activity. The difference in enzyme activity was found to be statistically significant ($p < 0.05$).

Calcite Dissolution Kinetics

Overall, the release of Ca^{2+} per unit time was greatest during the first 10 min. Thereafter, the reaction slowed gradually until equilibrium was achieved. The standard deviation ($<5\%$) for replicate determinations was very small indicating that relatively high accuracy during the entire experimental process. At any time, the order of the dissolution rate from largest to smallest was BCA, CA4 and CA0. The curves in Figure 4 show that calcite dissolution reached equilibrium in 240 min. Figure 5A shows that initially the particle surfaces were essentially free of organic material. Figure 5B shows that, subsequently, the particle surfaces became covered with organic matter.

Discussion

We tried to prepare growth curves with *B. mucilaginosus* in the presence and absence of calcite. However, the large amount of exopolysaccharide formed by this strain (Deng et al. 2003; Lian et al. 2008a) prevented precise determinations of growth by this organism. At first, there were only a few bacterial cells. Upon continued incubation of the culture,
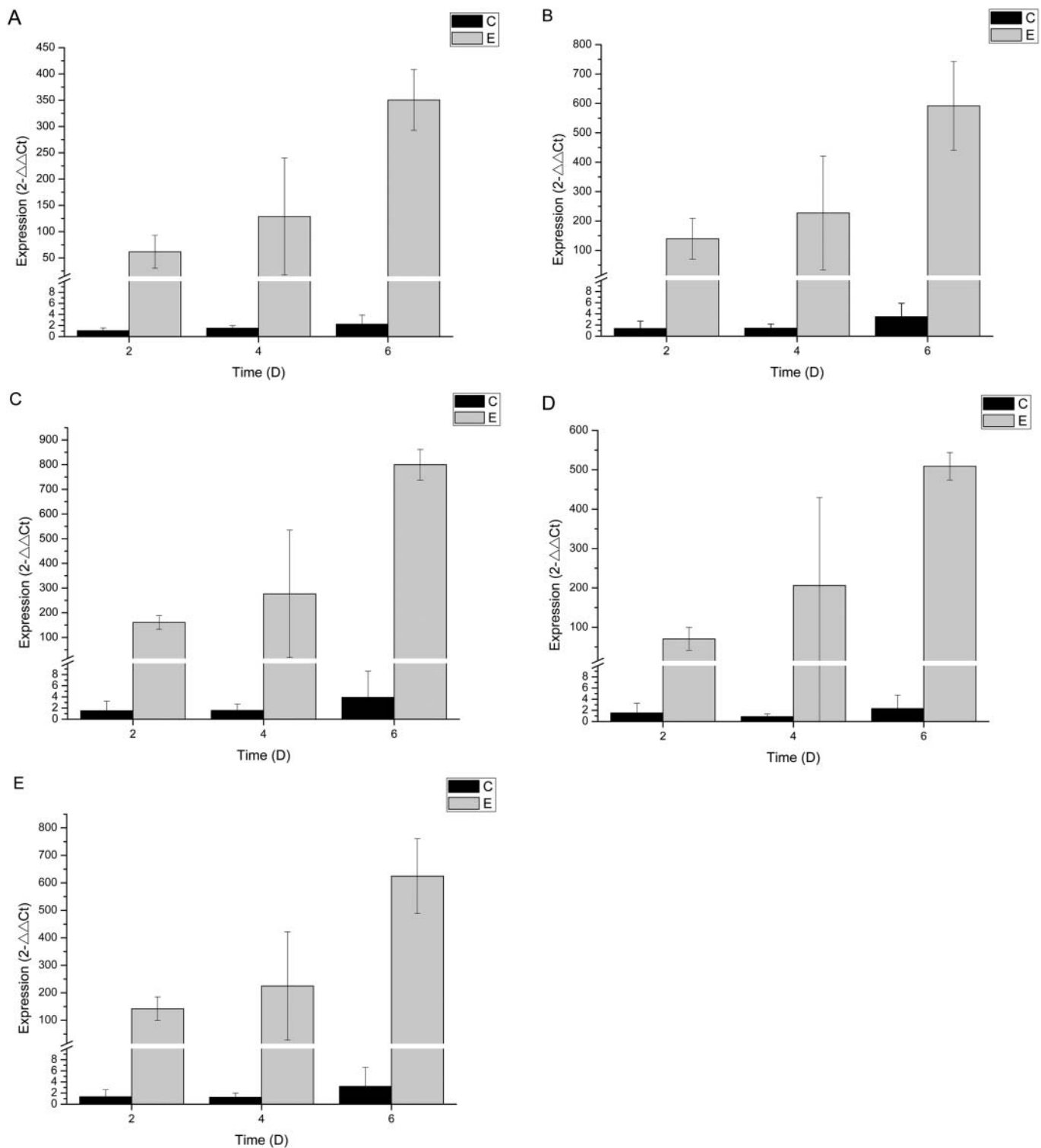
Fig. 1. mRNA relative expression quantities of different CA genes. (A), (B), (C), (D), and (E) show the expressions of gene1, gene2, gene3, gene4 and gene5, respectively. C and E represent the control and experimental groups. The calcium resource in the C and E group is $CaCl_2$ and calcite, respectively.

the cell population gradually increased. Thereafter, the increased extracellular polysaccharide had trapped calcite particles to such an extent as to slow down the rate of calcite dissolution. As a result, calcium ions needed for growth

became less available to the bacteria. In addition, because of local degradation of extracellular polymer of aerobic heterotrophic microorganisms, the alkalinity of the (micro)-environment may be elevated to accelerate the precipitation
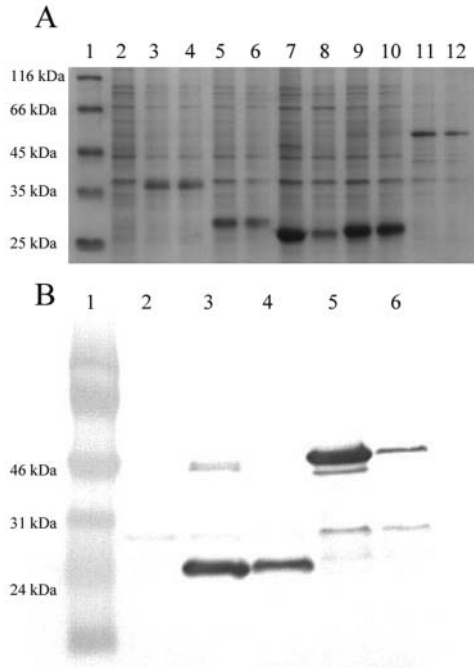
Fig. 2. Protein expression. (A) SDS-PAGE analysis of CA genes expression in *E. coli* Lanes: 1, molecular size marker; 2, negative control pET30a(+) in *E. coli* BL21 after IPTG induction; 3, total protein expressed in BL21 containing pXLL01; 4, the supernatant protein of lane 3; 5, total protein expressed in BL21 containing pXLL02; 6, supernatant protein of lane 5; 7, total protein expressed in BL21 containing pXLL03; 8, supernatant protein of lane 7; 9, total protein expressed in BL21 containing pXLL04; 10, supernatant protein of lane 9; 11, total protein expressed in BL21 containing pXLL05; 12, supernatant protein of lane 11. (B) Western blotting analysis CA genes expression in *E. coli*. Lanes: 1, molecular size marker; 2, negative control pET30a(+); 3, the total protein expressed in BL21 containing pXLL03; 4, the supernatant protein of lane 3; 5, the total protein expressed in BL21 containing pXLL05; 6, the supernatant protein of lane 5. The protein bands indicated by arrows show non-specific binding.

of $CaCO_3$ (Dupraz and Visscher 2005). The stress of limitation in calcium availability caused the bacteria to synthesize more CA to facilitate calcite dissolution. In the control cultures, sufficient dissolved calcium was still available, so that growth was not limited. The REL of the control, which was almost constant over time, was significantly lower than that of the experimental cultures.

This experiment provides direct evidence that calcite can promote the expression of CA genes in *B. mucilaginosus*. It implies a causal connection linking the expression of CA genes and the process of calcium utilization (Figure 6). Translated protein accelerated CO_2 hydration and produced an acidic environment that favored the dissolution of calcite. Although previous studies (Li et al. 2005a; Li et al. 2007) have shown that CA from microorganisms can play a role in mineral dissolution, some of the isozymes, which may not participate in mineral weathering, have a central role in bacterial metabolism. We have shown, in the present study, that
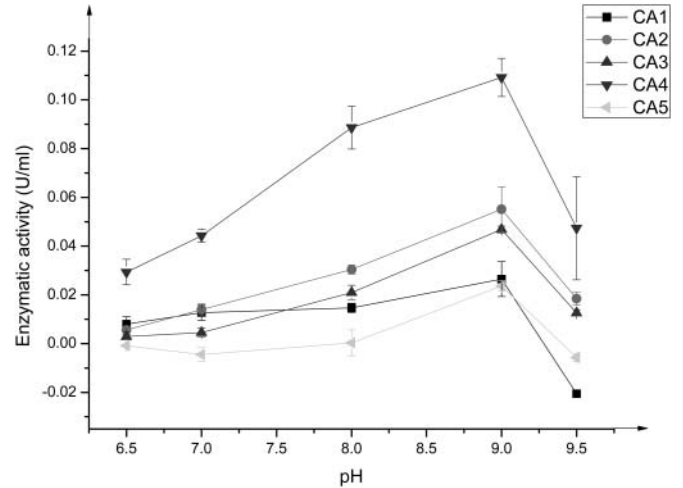

Fig. 3. CA activity of different crude enzyme solutions: relative enzymatic activity of CA at different pH values.

all five CA genes significantly up-regulated the production of corresponding enzyme proteins for playing a supplementary role in the promotion of calcite weathering in response to Ca^{2+} limitation.

To further determine whether CA has a role in promoting $CaCO_3$ dissolution, the gene for each of the CAs was cloned. The heterologously expressed proteins were generated and their activity determined. All the different CA proteins were active. This showed that our cloning method is applicable to the study of single CA gene expression. The ability of *B. mucilaginosus* to produce isozymes allows it to respond to some unfavorable environmental changes without negative effects on its metabolism. This phenomenon merits in-depth study to explain why so many CA genes co-exist in one species and what a central function each kind of CA plays. In
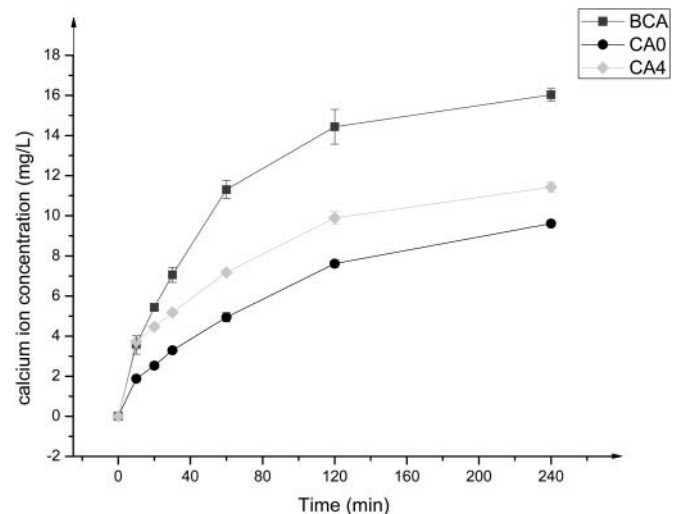

Fig. 4. Calcium ion concentrations at different times after the addition of different materials. BCA, CA0 and CA4 groups represent the reaction system adding BCA, CA0, and CA4, respectively.
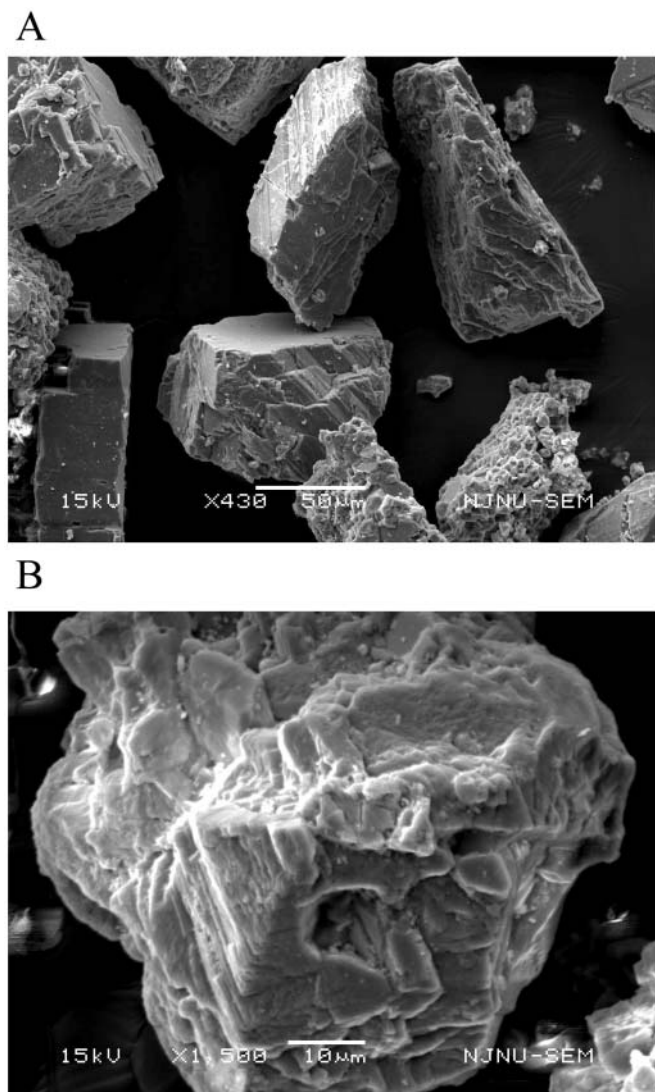
A

B

Fig. 5. SEM images of calcite particles after the dissolution reaction. (A) Calcite morphology in the CA4 group, 5 min; (B) particle morphology in the CA4 group, 180 min.

addition, the determination of enzymatic activity may serve as the basis for follow-up calcite dissolution experiments.

CA catalyzes the hydration of CO_2 leading to the formation of carbonic acid, regardless of whether the CO_2 is of atmospheric or metabolic origin. Dissociation of the carbonic acid yields H^+, which favors dissolution of $CaCO_3$. Calcite dissolution is determined in term of the overall reaction $(CaCO_3 + CO_2 + H_2O \Rightarrow Ca^{2+} + 2HCO_3^-)$. Stoichiometry requires that one molecule of CO_2 be converted to H^+ and HCO_3^- for each molecule of Ca^{2+} released. During the calcite dissolution, the following relation holds: $V\frac{d[CO_2]}{dt} = AR$ (Buhmann and Dreybrodt 1985; Dreybrodt et al. 1996). Here $[CO_2]$, V and A represent the concentrations of CO_2, the volume of the solution and the area of the mineral surface, respectively, and R is the flux of Ca^{2+} from the calcite surface and depends upon the chemical composition of the reaction system.

The release of Ca^{2+} per unit time was greatest during the first 10 min and the rate of dissolution in the CA4 group slowed down after the first 10 min compared with the BCA group (Figure 4). Figure 5 shows that, initially, the calcite particles had no organic deposit on them but did have such deposits 180 min after the start of the dissolution experiment. Coating the calcite particles in certain organic substances caused decreases in the dissolution rate over time (Luttge and Conrad 2004). At relatively small V/A ratios, the rate of dissolution was mainly affected by the conversion of CO_2 (Dreybrodt et al. 1996). During the first 10 min, the amount of Ca^{2+} released was higher in the CA4 group than in the CA0 group, and the dissolution rate was almost the same with BCA (Figure 4). This showed that CA protein from *B. mucilaginosus* CA gene transcription *in vitro* promoted calcite dissolution.

A pseudo–second-order kinetic model (Ho and Ofomaja 2006) was constructed for description of the dissolution behavior of calcite particles after 10 min:

$$\frac{t}{q_t} = \frac{1}{kq_e^2} + \frac{1}{q_e}t$$

Here, t is time, q_t is the quantity of Ca^{2+} released at a given time, k is the rate of Ca^{2+} release, and q_e is the equilibrium concentration of Ca^{2+}. A pseudo–second-order kinetic model of calcite dissolution is shown in Table 1. Although the surfaces of the calcite particles became covered in biofilm-like organic matter (Figure 5B), which inhibited dissolution to some extent, CA continued to play a certain role in weathering. The K value of the CA4 group was greater than that of the CA0 group. When equilibrium is reached, the q_e of the CA4 group was roughly equal to that of the CA0 group. This is consistent with the theory that enzymes do not change the

Table 1. Pseudo–second-order kinetic model of calcite dissolution

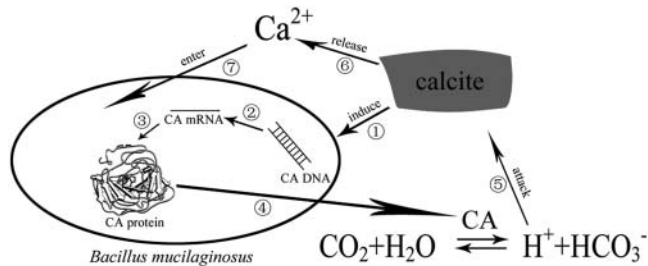| Group	Model	Equation	q_e (mg*L^{-1})	k (mg*L^{-1}*min^{-1})	R^2
BCA		$\frac{t}{q_t} = 5.060 + 0.0425t$	19.42	152.6	0.996
CA0	$\frac{t}{q_t} = \frac{1}{kq_e^2} + \frac{1}{q_e}t$	$\frac{t}{q_t} = 6.124 + 0.0794t$	12.60	25.90	0.981
CA4		$\frac{t}{q_t} = 2.979 + 0.0760t$	13.16	58.12	0.990

Fig. 6. An simulated diagram of a causal connection linking the expression of CA genes and the process of calcium utilization.

equilibrium point but only increase the rate of the reaction. The q_e of CA4 and CA0 was lower than that of the BCA group. Two reasons for this may be that: (I) some particles may be isolated when they become coated in organic matter, and (II) organic matter may be suitable for the regeneration of $CaCO_3$ at the heterologous nucleation sites, which leads to the formation of a secondary precipitate consuming Ca^{2+} in solution. The reaction may be described as follows:

$$Ca^{2+} + 2HCO_3{}^- \Rightarrow CaCO_3\downarrow + CO_2 + H_2O \quad \text{or}$$
$$Ca^{2+} + CO_3{}^{2-} \Rightarrow CaCO_3\downarrow$$
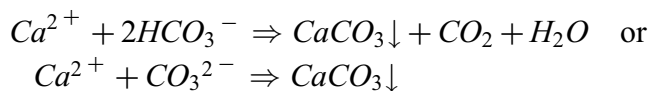
This shows that heterologously expressed CA proteins can promote calcite dissolution, which suggests that it may be feasible to solve geochemical problems using molecular biology. The current project provides a new perspective on mineral weathering and a foundation for further research into the role of microbial CA in the biogeochemical cycle. CA can promote mineral dissolution by increasing the reaction rate. Microorganisms can enhance their viability in the mineral-nutrient-poor environments by obtaining mineral elements in a timely manner through the auxiliary function of CA.

However, many studies (Kump et al. 2000; Ludwig et al. 1999) have not taken the role of enzyme catalysis in the mineral weathering process into account. This has caused the role of microorganisms in mineral weathering to be underestimated. In this way, our experimental results pose two questions worth studying in-depth: (I) whether all the CAs of the microbes play a supplemental role in mineral weathering; and (II) whether microbial mineral weathering from secreted enzymes will accelerate the carbon cycle as global concentrations of CO_2 increase.

Conclusions

RT-qPCR and heterologous expression analysis were used to study the relations of gene expression, calcite dissolution and the acquisition of Ca nutrition. RT-qPCR showed that calcite up-regulated the expression of CA genes and fostered the synthesis of CAs, which, in turn, promoted calcite dissolution. Heterologous expression of five types of CA products in

E. coli, determined by *B. mucilaginosus* CA gene sequences, were demonstrated to possess CA activity, and one type was shown to have the function of promoting calcite dissolution. These findings provide direct evidence that CAs from *B. mucilaginosus* play an auxiliary role in calcite weathering and Ca nutrition release under the condition of Ca^{2+} deficiency, which is conducive to the survival of bacteria.

Supplemental Material

Supplemental data for this article can be accessed on the publisher's website.

References

Alekseev A, Alekseeva T, Ostroumov V, Siegert C, Gradusov B. 2003. Mineral transformations in permafrost-affected soils, North Kolyma Lowland, Russia. Soil Sci Soc Am J 67:596–605.

Bahn YS, Cox GM, Perfect JR, Heitman J. 2005. Carbonic anhydrase and CO_2 sensing during *Cryptoloccus neoformans* growth, differentiation, and virulence. Curr Biol 15:2013–2020.

Banerjee S, Salunkhe SS, Apte-Deshpande AD, Mandi NS, Mandal G, Padmanabhan, S. 2009. Over-expression of proteins using a modified pBAD24 vector in *E. coli* expression system. Biotechnol Lett 31:1031–1036.

Bonneville S, Morgan DJ, Schmalenberger A, Bray A, Brown A, Banwart SA, Benning LG. 2011. Tree-mycorrhiza symbiosis accelerate mineral weathering: Evidences from nanometer-scale elemental fluxes at the hypha-mineral interface. Geochim Cosmochim Acta 75:6988–7005.

Bradfield JR. 1947. Plant carbonic anhydrase. Nature 159:467.

Brown DJ, Helmke PA, Clayton MK. 2003. Robust geochemical indices for redox and weathering on a granitic laterite landscape in central Uganda. Geochim Cosmochim Acta 67:2711–2723.

Buhmann D, Dreybrodt W. 1985. The kinetics of calcite dissolution and precipitation in geologically relevant situations of karst areas: 1. Open system. Chem Geol 48:189–211.

Chen J, Blume HP, Beyer L. 2000. Weathering of rocks induced by lichen colonization—A review. Catena 39:121–146.

Demir N, Nadaroglu H, Demir Y, Karaca S. 2012. Dissolution of dolomite and magnesite by catalysis of carbonic anhydrase and apocarbonic anhydrase. Ener Educ Sci Tech-A 28:853–860.

Deng S, Bai R, Hu X, Luo Q. 2003. Characteristics of a bioflocculant produced by *Bacillus mucilaginosus* and its use in starch wastewater treatment. Appl Microbiol Biotechnol 60:588–593.

Dreybrodt W, Lauckner J, Liu ZH, Svensson U, Buhmann D. 1996. The kinetics of the reaction $CO_2 + H_2O \rightarrow H^+ + HCO_3{}^-$ as one of the

rate limiting steps for the dissolution of calcite in the system H_2O-CO_2-$CaCO_3$. Geochim Cosmochim Acta 60:3375–3381.

Dupraz C, Visscher PT. 2005. Microbial lithification in marine stromatolites and hypersaline mats. Trends Microbiol 13:429–438.

Fru EC. 2011. Copper Bbiogeochemistry: A cornerstone in aerobic methanotrophic bacterial ecology and activity? Geomicrobiol J 28:601–614.

Godderis Y, Williams JZ, Schott J, Pollard D, Brantley SL. 2010. Time evolution of the mineralogical composition of Mississippi Valley loess over the last 10 kyr: Climate and geochemical modeling. Geochim Cosmochim Acta 74:6357–6374.

Hazen RM, Papineau D, Bleeker W, Downs RT, Ferry JM, McCoy TJ, Sverjensky DA, Yang H. 2008. Mineral evolution. Amer Mineral 93:1693–1720.

Hewett-Emmett D, Tashian RE. 1996. Functional diversity, conservation, and convergence in the evolution of the alpha-, beta-, and gamma-carbonic anhydrase gene families. Mol Phylogenet Evol 5:50–77.

Ho YS, Ofomaja AE. 2006. Pseudo-second-order model for lead ion sorption from aqueous solutions onto palm kernel fiber. J Hazard Mater 129:137–142.

Iskandar HM, Simpson RS, Casu RE, Bonnett GD, Maclean DJ, Manners JM. 2004. Comparison of reference genes for quantitative real-time polymerase chain reaction analysis of gene expression. Plant Mol Biol Rep 22:325–337.

Jackson DJ, Macis L, Reitner J, Degnan BM, Worheide G. 2007. Sponge paleogenomics reveals an ancient role for carbonic anhydrase in skeletogenesis. Science 316:1893–1895.

Jacobson AD, Wu LL. 2009. Microbial dissolution of calcite at T = 28 C and ambient pCO_2. Geochim Cosmochim Acta 73:2314–2331.

Koretsky C. 2000. The significance of surface complexation reactions in hydrologic systems: A geochemist's perspective. J Hydrol 230:127–171.

Kump LR, Brantley SL, Arthur MA. 2000. Chemical, weathering, atmospheric CO_2, and climate. Annu Rev Earth Pl Sci 28:611–667.

Lepleux C, Turpault MP, Oger P, Frey-Klett P, Uroz S. 2012. Correlation of the abundance of Betaproteobacteria on mineral surfaces with mineral weathering in forest soils. Appl Environ Microb 78:7114–7119.

Li W, Yu LJ, He QF, Wu Y, Yuan DX, Cao JH. 2005a. Effects of microbes and their carbonic anhydrase on Ca^{2+} and Mg^{2+} migration in column-built leached soil-limestone karst systems. Appl Soil Ecol 29:274–281.

Li W, Yu LJ, Wu Y, Jia LP, Yuan DX. 2007. Enhancement of Ca^{2+} release from limestone by microbial extracellular carbonic anhydrase. Bioresource Technol 98:950–953.

Li W, Yu LJ, Yuan DX, Wu Y, Zeng XD. 2005b. A study of the activity and ecological significance of carbonic anhydrase from soil and its microbes from different karst ecosystems of Southwest China. Plant Soil 272:133–141.

Li, W., Zhou, P.P., Jia, L.P., Yu, L.J., Li, X.L., Zhu, M., 2009. Limestone dissolution induced by fungal mycelia, acidic materials, and carbonic anhydrase from fungi. Mycopathologia 167:37–46.

Lian B, Chen Y, Zhao J, Teng HH, Zhu L, Yuan S. 2008a. Microbial flocculation by *Bacillus mucilaginosus*: Applications and mechanisms. Bioresour Technol 99:4825–4831.

Lian B, Wang B, Pan M, Liu CQ, Teng HH. 2008b. Microbial release of potassium from K-bearing minerals by thermophilic fungus *Aspergillus fumigatus*. Geochim Cosmochim Acta 72:87–98.

Liu ZH, Yuan DX, Dreybrodt W. 2005. Comparative study of dissolution rate-determining mechanisms of limestone and dolomite. Environ Geol 49:274–279.

Ludwig W, Amiotte-Suchet P, Probst J-L. 1999. Enhanced chemical weathering of rocks during the last glacial maximum: a sink for atmospheric CO_2? Chem Geol 159:147–161.

Luttge A, Conrad PG. 2004. Direct observation of microbial inhibition of calcite dissolution. Appl Environ Microb 70:1627–1632.

Mailloux BJ, Alexandrova E, Keimowitz AR, Wovkulich K, Freyer GA, Herron M, Stolz JF, Kenna TC, Pichler T, Polizzotto ML, Dong HL, Bishop M, Knappett PSK. 2009. Microbial mineral weathering for nutrient acquisition releases arsenic. Appl Environ Microb 75:2558–2565.

McMaster TJ. 2012. Atomic force microscopy of the fungi-mineral interface: applications in mineral dissolution, weathering and biogeochemistry. Curr Opin Biotech 23:562–569.

Meldrum NU, Roughton FJ. 1933. Carbonic anhydrase. Its preparation and properties. J Physiol 80:113–142.

Meunier A, Sardini P, Robinet JC, Pret D. 2007. The petrography of weathering processes: facts and outlooks. Clay Miner 42:415–435.

Mo BB, Lian B. 2011. Hg(II) adsorption by *Bacillus mucilaginosus*: mechanism and equilibrium parameters. World J Microbiol Biotechnol 27:1063–1070.

Moroney JV, Bartlett SG, Samuelsson G. 2001. Carbonic anhydrases in plants and algae. Plant Cell Environ 24:141–153.

Neaman A, Chorover J, Brantley SL. 2005. Implications of the evolution of organic acid moieties for basalt weathering over geological time. Am J Sci 305:147–185.

Nielsen SS. 2010. Complexometric Determination of Calcium, Food Analysis Laboratory Manual. New York: Springer, p61–67.

Niu C, Kebede H, Auld DL, Woodward JE, Burow G, Wright RJ. 2008. A safe inexpensive method to isolate high quality plant and fungal DNA in an open laboratory environment. Afr J Biotechnol 7:2818–2822.

Nolan T, Hands RE, Bustin SA. 2006. Quantification of mRNA using real-time RT-PCR. Nat Protoc 1:1559–1582.

Papamichael EM, Economou ED, Vaimakis TC. 2002. Dissolution of the carbonate minerals of phosphate ores: Catalysis by carbonic anhydrase II, from bovine erythrocytes, in acid solutions. J Coll Interf Sci 251:143–150.

Pocker Y, Stone JT. 1967. The catalytic versatility of erythrocyte carbonic anhydrase. 3. Kinetic studies of the enzyme-catalyzed hydrolysis of p-nitrophenyl acetate. Biochemistry-US 6:668–678.

Sambrook J, Russell DW. 2002. Molecular Cloning: A Laboratory Manual, 3rd ed. New York: Cold Spring Harbor Laboratory Press. p163.

Shelobolina E, Xu HF, Konishi H, Kukkadapu R, Wu T, Blothe M, Roden E. 2012. Microbial lithotrophic oxidation of structural Fe (II) in biotite. Appl Environ Microb 78:5746–5752.

Shirokova LS, Benezeth P, Pokrovsky OS, Gerard E, Menez B, Alfredsson H. 2012. Effect of the heterotrophic bacterium *Pseudomonas reactans* on olivine dissolution kinetics and implications for CO_2 storage in basalts. Geochim Cosmochim Acta 80:30–50.

Shock EL. 2009. Minerals as energy sources for microorganisms. Econ Geol 104:1235–1248.

Singh G, Biswas DR, Marwaha TS. 2010. Mobilization of potassium from waste mica by plant growth promoting rhizobacteria and its assimilation by maize (*zea mays*) and wheat (*Triticum aestivum l.*): A hydroponics study under phytotron growth chamber. J Plant Nutr 33:1236–1251.

Small E, Eggler A, Mesecar AD. 2010. Development of an efficient *E. coli* expression and purification system for a catalytically active, human Cullin3-RINGBox1 protein complex and elucidation of its quaternary structure with Keap1. Biochem Bioph Res Co 400:471–475.

Smith KS, Ferry JG. 2000. Prokaryotic carbonic anhydrases. FEMS Microbiol Rev 24:335–366.

Sorensen HP, Mortensen KK. 2005. Advanced genetic strategies for recombinant protein expression in *Escherichia coli*. J Biotechnol 115:113–128.

Stockmann GJ, Shirokova LS, Pokrovsky OS, Benezeth P, Bovet N, Gislason SR, Oelkers EH. 2012. Does the presence of heterotrophic

bacterium *Pseudomonas reactan*s affect basaltic glass dissolution rates? Chem Geol 296:1–18.

Sunderhaus S, Dudkina NV, Jansch L, Klodmann J, Heinemeyer J, Perales M, Zabaleta E, Boekema EJ, Braun HP. 2006. Carbonic anhydrase subunits form a matrix-exposed domain attached to the membrane arm of mitochondrial complex I in plants. J Biol Chem 281:6482–6488.

Supuran CT, Scozzafava A. 2007. Carbonic anhydrases as targets for medicinal chemistry. Bioorgan Med Chem 15:4336–4350.

Tripp BC, Smith K, Ferry JG. 2001. Carbonic anhydrase: new insights for an ancient enzyme. J Biol Chem 276:48615–48618.

Uroz S, Calvaruso C, Turpaul MP, Pierrat JC, Mustin C, Frey-Klett P. 2007. Effect of the mycorrhizosphere on the genotypic and metabolic diversity of the bacterial communities involved in mineral weathering in a forest soil. Appl Environ Microb 73:3019–3027.

Valix M, Usai F, Malik R. 2001. Fungal big-leaching of low grade laterite ores. Miner Eng 14:197–203.

Venta PJ, Shows TB, Curtis PJ, Tashian RE. 1983. Polymorphic gene for human carbonic anhydrase II: a molecular disease marker located on chromosome 8. Proc Natl Acad Sci 80:4437–4440.

Warscheid T, Braams J. 2000. Biodeterioration of stone: a review. Inter Biodeterior Biodegrad 46:343–368.

Wilson MJ. 2004. Weathering of the primary rock-forming minerals: Processes, products and rates. Clay Miner 39:233–266.

Xiao B, Lian B, Shao WL. 2012a. Do bacterial secreted proteins play a role in the weathering of potassium-bearing rock powder? Geomicrobiol J 29:497–505.

Xiao B, Lian B, Sun LL, Shao WL. 2012b. Gene transcription response to weathering of K-bearing minerals by *Aspergillus fumigatus*. Chem Geol 306:1–9.

Xu Y, Feng L, Jeffrey PD, Shi YG, Morel FMM. 2008. Structure and metal exchange in the cadmium carbonic anhydrase of marine diatoms. Nature 452:56–61.

Zhang ZC, Lian B, Hou WG, Chen MX, Li X, Li Y. 2011. Bacillus mucilaginosus can capture atmospheric CO_2 by carbonic anhydrase. Afr J Microbiol Res 5:106–112.